Interpolated potential energy surface and classical dynamics for H 3 + + HD and H 3 + + D 2

Gloria E. Moyano and Michael A. Collins

Citation: The Journal of Chemical Physics **119**, 5510 (2003); doi: 10.1063/1.1599339
View online: http://dx.doi.org/10.1063/1.1599339
View Table of Contents: http://scitation.aip.org/content/aip/journal/jcp/119/11?ver=pdfcov
Published by the AIP Publishing

Interpolated potential energy surface and classical dynamics for $H_3^+ + HD$ and $H_3^+ + D_2$

Gloria E. Moyano and Michael A. Collins[a)]
Research School of Chemistry, Australian National University, Canberra, ACT 0200, Australia

(Received 4 April 2003; accepted 18 June 2003)

A potential energy surface for H_5^+ has been constructed by a modified Shepard interpolation on a sparse set of data points, using second order Möller–Plesset perturbation theory. An improved version of the surface was also obtained by substituting the energy values at the data points with values evaluated using a coupled cluster treatment (with single and double excitations, and perturbative treatment of triple excitations). Classical simulations for the collisions between $H_3^+ + HD$ and $H_3^+ + D_2$ were carried out in order to calculate the total integral cross sections and rate coefficients for these systems. There is good agreement with earlier experimental data for rate coefficients at temperatures between 80 and 300 K, but the predicted rate coefficient for the reaction of $H_3^+ + HD$ at 10 K deviates from the most recent experimental measurement, suggesting that quantum rather than classical reaction dynamics are necessary. © *2003 American Institute of Physics.* [DOI: 10.1063/1.1599339]

I. INTRODUCTION

Deuterium is present in the universe in a relatively low amount. An elemental D/H ratio of 2×10^{-5} applies to much of our galaxy,[1] and in the interstellar medium (ISM) deuterium occurs mostly in the HD molecular form.[2,3] Nevertheless, deuterium takes an active part in interstellar chemistry, leading to an enhancement of the abundances of deuterated molecules. In interstellar clouds, such processes are known as deuterium fractionation;[2] the most relevant of them are thought to be gas phase ion–molecule reactions. Specifically, the reaction

$$H_3^+ + HD \rightarrow H_2D^+ + H_2 \tag{1.1}$$

has been pointed out as the principal deuterium fractionation source in the ISM, and HD, H_2D^+, CH_2D^+, and C_2HD^+ as the dominant molecules in ISM deuterium chemistry (see references cited in Refs. 3 and 4).

Accurate values for the rate coefficients of deuterium fractionation reactions are necessary to validate hypotheses concerning interstellar deuterium chemistry. Several experimental studies of those reactions have been performed in the past (see, e.g., Refs. 5–8), but measurements at the typical temperatures of interstellar clouds ($T\sim10\,\mathrm{K}$) have been performed only very recently.[9] The most recent values for the rate coefficient for reaction (1.1), and for related ion–molecule gas phase reactions, are considerably below the expected Langevin value and earlier results.[3,9] Furthermore, comparisons of predicted and observed values for the amount of deuterium fractionation in some dark clouds have been used to support the suggestion that ion–molecule gas phase reactions are less efficient than had been expected. Hence, it has been proposed that other mechanisms should also play an important role in deuterium fractionation.[10]

The purpose of this paper is to provide an accurate molecular potential energy surface (PES) for this system, so that accurate theoretical rate coefficients can be evaluated for reaction (1.1) and isotopic analogs. The classical reaction dynamics is also reported. Previous theoretical treatments of the deuterium fractionation reactions have followed various approaches. *Ab initio* quantum studies have been focused on some molecular configurations and reaction paths,[11–17] and the Langevin model has been employed for kinetics. The construction of a very accurate *ab initio* potential energy surfaces (PES) for H_5^+ dynamics has remained a challenge.[18,19] In fact, a very recent paper[9] underlines the lack of collision dynamics treatments to compare with the experimental data for reactive systems like that in Eq. (1.1).

An accurate PES can now be constructed by interpolation of *ab initio* energies and energy derivatives for configurations scattered over regions relevant to the dynamics of unimolecular and bimolecular reactions.[20–23] This type of PES is constructed with the aid of classical trajectory simulations of the reaction dynamics. Hence, we also report classical dynamics calculations of reaction probabilities, cross sections and rate coefficients for reaction (1.1) and the isotopic variants,

$$H_3^+ + D_2 \rightarrow HD_2^+ + H_2 \tag{1.2}$$

$$\rightarrow H_2D^+ + HD. \tag{1.3}$$

It has been proposed that reactions like (1.1) and isotopic analogs follow a mechanism in which metastable H_5^+ (or isotopic variants) intermediates can be formed, so that hydrogen/isotope exchange occurs by isomerization (see, e.g., Ref. 7). Structural features of H_5^+ clusters have been studied in detail by means of a range of quantum methods.[11–18] As expected for cluster systems, the H_5^+ PES has shown a large number of stationary points, from which at least ten of the lowest energy structures have been found and

a)Electronic mail: collins@rsc.anu.edu.au

characterized. Very high levels of approximation and large basis sets have been employed,[14,15,18] taking into account the fact that the energy differences between the different H_5^+ structures are very small and correlation effects are determinant for quantitative agreement with experimental thermodynamics data.[12,17] At the minimum energy configuration known for H_5^+, established through vibrational analysis,[13,15,18] the C_{2v} symmetry cluster looks like an H_3^+ ion loosely bound to an H_2 molecule. The role of this ion–molecule complex in the reaction mechanism has been investigated here using classical trajectory simulations.

The reaction mechanism observed in the simulations is compared with the Langevin model as well as with the experimental results at low temperatures. The need for accurate quantum scattering calculations is discussed in the light of these results.

Section II of this paper consists of a summary of the PES construction method and *ab initio* quantum calculations involved. Section III presents the numerical results and discussion of the theoretical treatment of reactions (1.1)–(1.3). Section IV contains a summary and concluding remarks.

II. METHODS

A. Potential energy surface for H_5^+

The details of the construction of interpolated PES for systems of more than four atoms have been presented previously.[20,22,23] In brief, the PES takes the form,

$$E(\mathbf{Z}) = \sum_{g \in G} \sum_{i=1}^{N_{\text{data}}} w_{g \circ i}(\mathbf{Z}) T_{g \circ i}(\mathbf{Z}), \tag{2.1}$$

in which a number N_{data} of local Taylor expansions T_i of the energy, around certain molecular configurations, are combined as a weighted average. These N_{data} molecular configurations are referred to below as the ''data set.'' The Taylor expansions are evaluated from *ab initio* calculation of the energies and up to energy second derivatives at each of the N_{data} configurations. Each expansion is expressed in terms of a geometry-specific set of $3N-6$ independent coordinates which are linear combinations of the inverse interatomic distances, $\mathbf{Z}=\{Z_1,\ldots,Z_k,\ldots,Z_{N(N-1)/2}\}$, where $Z_k=1/R_k$. For H_5^+ we have $N=5$ atoms and so a total of 10 Z coordinates. The sum over $g \in G$ in Eq. (2.1) means that the data set includes all possible equivalents of a configuration by permutation of identical nuclei (120 in the case of H_5^+), so that the PES is symmetric with respect to permutations of the hydrogens.

In simple terms, the weight function w_i in Eq. (2.1) depends on the distance from $\mathbf{Z}$ to the data point configuration $\mathbf{Z}(i)$, and estimated ''confidence lengths'' for each data point.[20,23] The confidence lengths were evaluated using an energy tolerance, $E_{\text{tol}}=1.31$ kJ/mol, and energy gradients at $M=100$ data points (see Ref. 23 for definitions of E_{tol} and M). The data set is built up by an iterative procedure in which classical trajectories are used to sample the relevant regions of configuration space. The construction of the PES and classical trajectory simulations were performed with the program suite GROW.[20]

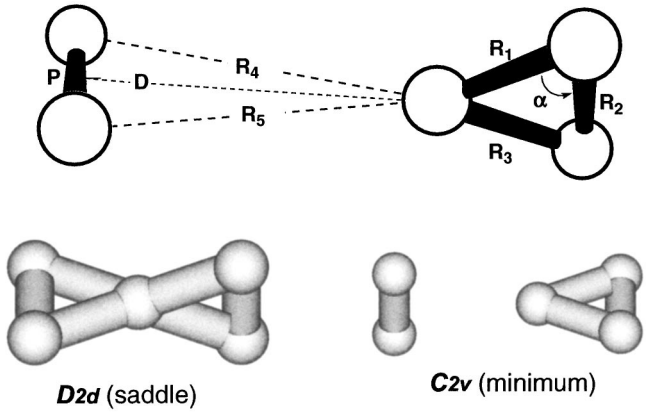

FIG. 1. Definitions of the geometrical parameters for the H_5^+ complex and structure representations of the two lowest energy stationary points. In both the D_{2d} and C_{2v} configurations, the vertices involved in the definition of the angle α lie in a plane perpendicular to the distance segment P.

This program constructs the PES of Eq. (2.1) in an iterative fashion. An initial data set of configurations is chosen on intuitive grounds, usually as locations on a relevant reaction path. The PES of Eq. (2.1), with this initial data set, is used to perform a classical simulation of the reaction with a few (say ten) trajectories. Molecular configurations encountered in this simulation are temporarily stored as a sample of the dynamically important molecular configurations. One of these configurations is selected to be a new data point. The automated selection process has been described elsewhere.[20] With the addition of one data point, the PES is altered. The cycle of trajectory simulation, sampling and selection is repeated to produce one more data point. The process is iterated at least hundreds of times until the PES is deemed to be converged. Convergence is demonstrated when large scale trajectory simulation of the reaction cross section (or other relevant observable) shows no significant dependence on the size of the data set.

B. *Ab initio* methods and initial configurations

There have been several previous high level *ab initio* studies of H_5^+.[11–17] About ten stationary points have been identified and characterized on the PES.[11,15,18] The only minimum is a C_{2v} symmetry structure as shown in Fig. 1. Tables I and II summarize the structure and energy of this minimum as determined here and by earlier authors. It is clear that the energy and structure of this minimum is quite accurately described at the second order Møller–Plesset perturbation [MP2/6-311G(d,p)] level of approximation by comparison with the most reliable treatments of electron correlation and largest basis sets. The first order D_{2d} symmetry saddle point (see Fig. 1), which separates two equivalent minima is the lowest barrier to rearrangement within the H_5^+ complex. The barrier height relative to the minimum is also accurately described at the MP2/6-311G(d,p) level (see Table II).

The H_5^+ clusters are weakly bound. The most accurate *ab initio* methods employed predict an energy change for reaction,

TABLE I. Geometrical parameters[a] for the two, C_{2v} and D_{2d}, lowest energy H_5^+ stationary points, and the $H_3^+ + H_2$ minimum at different *ab initio* levels of approximation.

	MP2 6-311G(d,p)			CCSD(T)-R12 $7s4p3d$[b]		CISD $6s3p$[c]			QCISD(T) cc-pVQZ[d]		
	C_{2v}	D_{2d}	$H_3^+ + H_2$	C_{2v}	D_{2d}	C_{2v}	D_{2d}	$H_3^+ + H_2$	C_{2v}	D_{2d}	$H_3^+ + H_2$
P (Å)	0.7649	0.7821	0.7383	0.765	0.780	0.7640	0.784	0.7433	0.76620	0.76620	0.7419
D (Å)	1.2517	1.0541	∞	1.324	1.054	1.3387	1.054	∞	1.29177	1.05436	∞
R_1 (Å)	0.9935	1.1243	0.8740	0.966	1.125	0.9606	1.124	0.8752	0.97704	1.12502	0.8737
R_2 (Å)	0.8061	0.7821	0.8740	0.816	0.780	0.8174	0.784	0.8752	0.81266	0.78487	0.8737
α (deg)	66.07	69.65	60.0	65.0	69.6	64.82	69.6	60.0	65.4	69.6	60.0

[a]For definitions of the symbols P, D, R_1, α, and R_2 see Fig. 1.
[b]Reference 14.
[c]Reference 15.
[d]Reference 18.

$$H_5^+ \rightarrow H_3^+ + H_2 \tag{2.2}$$

in the range 21–25 kJ mol^{-1} [20.94 kJ mol^{-1} is the MP2 6-311G(d,p) value for the dissociation energy in reaction (2.2)]. Furthermore, the energies calculated for the other stationary points known for H_5^+ show that rearrangement barriers within the complex are as low as 0.7–2 kJ mol^{-1}.[18] From the chemical point of view, we can consider the PES for the H_5^+ system as almost flat in the region of the minimum.

Experimental values for the enthalpy of reaction (2.2) determined over the last 30 years have shown considerable variation due to different factors affecting the measurements (see a discussion in Ref. 24). The recent ΔH^0 (25–330 K) values determined by Hiraoka and co-workers 28.9±1.3 kJ mol^{-1},[24] and 29.3±0.4 kJ mol^{-1},[25] have been taken here as reference for comparison. The dissociation energies (D_0) calculated at very high *ab initio* levels (summarized in Table II) are not in quantitative agreement with such experimental values, but the difference has been attributed mainly to thermal contributions,[12,16] as well as to the inadequacy of the harmonic approximation in the vicinity of the C_{2v} H_5^+ minimum. More refined calculations of the zero point vibrational energy (ZPVE) correction based on a model Hamiltonian for the nuclear dynamics,[19] and an estimation of the thermal corrections at 298.15 K (Ref. 12) reduce the difference between theoretical and experimental data. Nevertheless, it can be seen in Table II that the MP2/6-311G(d,p) value for D_0 is in good agreement with the predictions of the most reliable *ab initio* quantum chemistry methods employed so far.

TABLE II. Relative energies[a] in kJ mol^{-1} for the two C_{2v} and D_{2d} lowest energy H_5^+ stationary points, and dissociation energy D_0 according to reaction (2.2), at different *ab initio* levels of approximation.

	MP2 6-311G(d,p)	CCSD(T) 6-311G(d,p)[b]	CCSD(T)-R12 $7s4p3d$[c]	CISD $6s3p$[d]	QCISD(T) cc-pVQZ[e]
C_{2v}	−32.21	−33.29	−35.65	−33.56	−35.70
D_{2d}	−31.74	−33.08	−34.89	−32.07	−34.94
D_0	20.94[f]	22.00[g]	25.5	20.96[f]	24.10[f]

[a]The reference energy corresponds to the asymptotic value for $H_3^+ + H_2$.
[b]Energy values calculated at the geometries of the MP2/6-311G(d,p) stationary points.
[c]Reference 14.
[d]Reference 15.
[e]Reference 18.
[f]Calculated using ZPVE correction in the harmonic approximation.
[g]Calculated using the CCSD(T)/6-311G(d,p) energy values and the MP2/6-311G(d,p) ZPVE correction in the harmonic approximation.

Since the global PES of Eq. (2.1) requires hundreds (or thousands) of data points (at which energies, gradients and second derivatives are required), we have chosen the MP2/6-311G(d,p) approximation as the most appropriate in terms of accuracy and computational cost. We denote this surface as the MP2 PES In order to improve the reliability of the constructed PES, the coupled cluster treatment with single and double excitations, and perturbative treatment of triple excitations [CCSD(T)/6-311G(d,p)] has been employed below to evaluate the energy (only) at each of the data set configurations. A new PES has then been constructed by simply replacing the energy of each data point by the CCSD(T)/6-311G(d,p) value. We denote this surface as the CCSD(T)-MP2 PES. A similar approach has been used to improve the accuracy of this type of PES in the H_3O system.[26] The relative energies of stationary points on the CCSD(T)-MP2 PES are also shown in Table II.

An initial data set for the PES was generated as follows. Beginning from the C_{2v} symmetry minimum, a dissociation path to H_3^+ and H_2 was determined. The D_{2d} symmetry saddle point, which connects two equivalent C_{2v} symmetry minima, was also found (see Fig. 1). A data set of 20 configurations was constructed, including the minimum, the D_{2d} saddle point, and geometries on the reaction path in which the H_2 fragment separates from the H_3^+ for up to 13.2 Å. All the *ab initio* quantum calculations in this work were carried out using the GAUSSIAN 98 package.[27]

C. Classical dynamics

Classical trajectory calculations for reactions (1.1)–(1.3) were performed during the iterative construction of the PES and also to evaluate the reaction cross sections. A velocity-Verlet integration algorithm[28] was used with a time step size of 1.0×10^{-17} s, and batches of trajectories were started from the asymptotes $H_3^+ + D_2$ and $H_3^+ + HD$, with a fragment to fragment center of mass separation of 13.2 Å. Trajectories were terminated when the separating fragments reached this distance.

During the PES growing process, data points added to the interpolating function were sampled mostly from trajectories started at $H_3^+ + D_2$, for relative kinetic energies of the

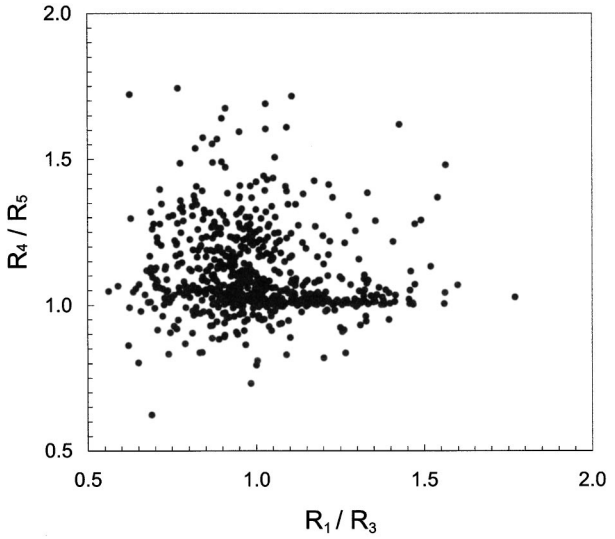

FIG. 2. Two-dimensional projection of data point configurations for the H_5^+ system. The 728 PES configurations, but not their equivalents by permutation, are illustrated. See Fig. 1 for definitions of distance parameters.

fragments of 5.0×10^{-4} and $7.5\times10^{-3}\,E_h$ and impact parameter $b=0$. The fragments were given zero rotational angular momentum and initial vibrational energies corresponding to their respective ZPVE levels ($7.43\times10^{-3}\,E_h$ for D_2, $9.10\times10^{-3}\,E_h$ for HD, and $2.1\times10^{-2}\,E_h$ for H_3^+); the initial atomic velocities and configurations for the reactants were generated using the efficient microcanonical sampling method of Schranz *et al.*[29] 88 data points were sampled from trajectories started at the D_{2d} first order saddle point for H_5^+.

To estimate reaction cross sections, batches of 999 trajectories, initiated at the asymptotes $H_3^+ + D_2$ and $H_3^+ + HD$, were run for several relative kinetic energies over the range from 7.5×10^{-4} to $5.0\times10^{-2}\,E_h$. Impact parameters b for those trajectories were sampled randomly from a distribution limited by a maximum exceeding the largest value at which reaction was obtained for that kinetic energy. The distributions of b values were such that the probability of a trajectory having an impact parameter between b and $b+db$ was proportional to b.

III. RESULTS AND DISCUSSION

A. Interpolated PES

The initial data set of 20 points was iteratively ''grown'' to 728 points. The distribution of these data points over the configuration space is indicated by the projection shown in Fig. 2. Convergence of the PES was established by estimating the total cross section for reactions (1.2)–(1.3) by trajectory simulation on a PES with the first 450, 550, 650, and 728 data points. The total cross sections for reactions (1.2)–(1.3) at a translational energy of $7.5\times10^{-3}\,E_h$ were found to be 22.14 ± 0.72 Å^2, 21.78 ± 0.72 Å^2, 21.78 ± 0.72 Å^2, and 21.75 ± 0.68 Å^2 for those four data sets, respectively. Note that if collisions of H_3^+ with H_2 were considered (particularly for vibrationally excited H_2) additional data points may be required to ensure convergence of the PES at the larger amplitude vibrations which would be involved.

As an additional test of the accuracy of the interpolation, MP2/6-311G(d,p) energies for 761 geometries sampled randomly from trajectory simulations were calculated and compared to the interpolated values. The average absolute difference for a PES with 728 points was approximately 0.4% of the energy range ($3.2\times10^{-2}\,E_h$) of the sampled configurations. This magnitude of error compares favorably with the errors observed in applications of this type of PES to other systems.

For the 728 data points, the energy difference between MP2 and CCSD(T) values shows a narrow normal distribution with an average of $-0.018\pm0.001\,E_h$. Therefore, the CCSD(T)-MP2 and the MP2 surfaces are very similar in shape. The binding energy D_e predicted for H_5^+ at the CCSD(T) level, according to reaction (2.2), increases by only 1.06 kJ mol^{-1} over the MP2 value at the MP2 geometries.

In addition, the total cross section for reaction (1.1) was calculated using both MP2 and CCSD(T) PESs at seven relative translational energies within the range 7.5×10^{-4}–$5.0\times10^{-2}\,E_h$. For every energy the two predicted cross sections were very close to each other as can be seen in Table III. The maximum difference between the MP2 and the CCSD(T)-MP2 PES based cross sections for reaction (1.1) is equivalent to two times the standard deviation for the statistics based on 999 trajectories at $1.0\times10^{-2}\,E_h$.

B. Reaction cross sections and rate constants

Figures 3 and 4 show the total reaction cross section for reaction (1.1) and reactions (1.2)–(1.3) respectively, as a function of the initial relative translational energy E_{tr} of the reactants.

The Langevin cross section, given by the formula[30]

$$\sigma=\pi\left(\frac{2e^2\alpha}{E_{tr}}\right)^{1/2} \tag{3.1}$$

is included in these figures for comparison. In Eq. (3.1), e denotes the ionic charge, and α the dipole polarizability of the neutral reactant (HD or D_2). The values used for the dipole polarizabilities of HD and D_2 in Eq. (3.1) were the values for the lowest vibrational and rotational states for these molecules as calculated by Rychlewski.[31]

TABLE III. Cross sections for reaction (1.1) at different relative translational energies of the reactants, calculated using the MP2 and CCSD(T)-MP2 PES.[a]

Energy (E_h)	7.5 (−4)	1.0 (−3)	5.0 (−3)	7.5 (−3)	1.0 (−2)	2.5 (−2)	5.0 (−2)
CCSD(T)-MP2 σ (Å^2)	64.05±1.83	56.47±1.68	27.22±0.89	21.41±0.72	16.96±0.59	10.36±0.41	6.76±0.32
MP2 σ (Å^2)	62.07±1.83	57.75±1.68	25.70±0.89	22.09±0.72	18.04±0.59	10.20±0.41	6.58±0.32

[a]Notation $x(-y)$ is used in this paper to represent $x\times10^{-y}$.

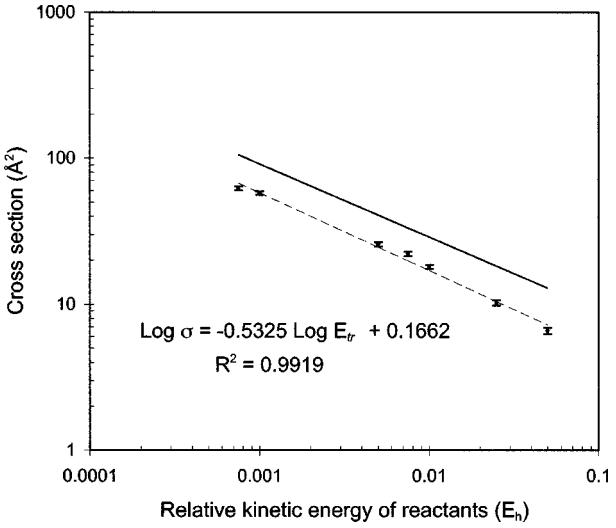

FIG. 3. Total cross section (●) as a function of the relative kinetic energy, E_{tr}, of the reactants for reaction (1.1). The error bars denote two standard deviations in the classical simulations. The solid line corresponds to the Langevin relationship (3.1), and the dashed line corresponds to the logarithmic relationship fitted to the classical cross sections (σ). R^2 is the coefficient of determination for the least squares regression.

The cross sections predicted using the interpolated PES follow a trend approximately linear with $(E_{\mathrm{tr}})^{-1/2}$ in both cases. A least squares fitting, using logarithmic scales for both variables, gives an average power for E_{tr} of -0.53 (for both systems), close to the value of -0.5 for the Langevin model. The trajectory cross sections are on average 59.7% of the Langevin values for $H_3^+ + D_2$, and 60.1% for $H_3^+ + HD$.

An experimental study of the energy dependence of the total cross section for reaction (1.2) was made by means of a merged molecular beam technique.[6] A close comparison with our results is not possible as the experimental conditions implied very high vibrational states for the reactants. However, it is noteworthy that over the range of E_{tr} considered in this work the observed energy dependence is similar to that predicted here. For higher values of E_{tr}, the experimental cross sections deviate significantly from the predicted trend and decrease very rapidly as the energy increases.[6]

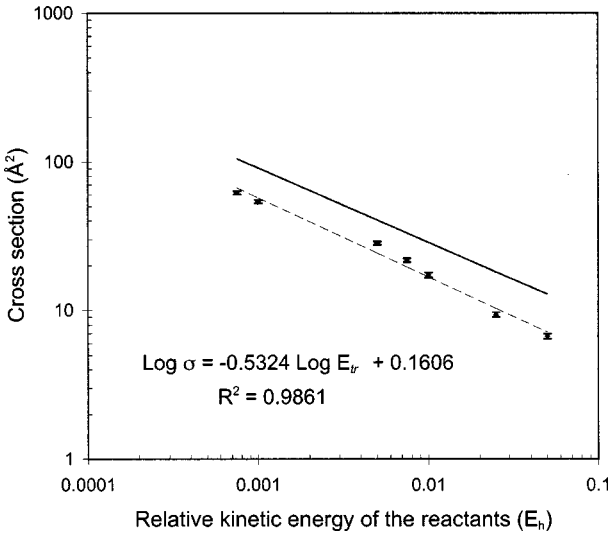

FIG. 4. As in Fig. 3, for the combined total cross sections of reactions (1.2) and (1.3).

TABLE IV. Total rate coefficients for the reaction of $H_3^+ + D_2$.

	k ($\mathrm{cm^3\,s^{-1}}$)			
T (K)	a	b	c	d
80	1.04 (−9)	9.95(−10)	1.4(−9)	1.1(−9)
300	9.99(−10)	9.64(−10)	1.3(−9)	1.0(−9)

[a]This work (using the MP2 PES); for combined reactions (1.2)–(1.3).
[b]This work (using the MP2 PES); for reaction (1.2) only.
[c]Experimental [for combined reactions (1.2) and (1.3)] uncertainty ±25%, see Ref. 7.
[d]Experimental [for reaction (1.2) only]; uncertainty ±10%, see Ref. 7.

To estimate the thermal rate coefficient for these reactions, the least squares fits for the cross sections, shown in the figures, have been integrated over a Maxwell–Boltzmann distribution of relative molecular velocities.[30] The calculated reaction rate coefficient, k, for the combined reactions (1.2)–(1.3) is shown on Table IV, along with experimental values determined at the same temperatures, using a variable temperature ion flow tube (VT-SIFT).[7] The Langevin model predicts a temperature independent rate coefficient of $1.59 \times 10^{-9}\,\mathrm{cm^3\,s^{-1}}$, for these combined reactions.

To compare values in Table IV, we have to take into account that the measurements can be affected by nonequilibration of the reactant species below 300 K in the VT-SIFT experiment.[7] On the other hand, our dynamics calculations were performed supposing zero total rotational angular moment for the reactants, rather than a thermal distribution. Nevertheless, there is good agreement between the calculated and the experimental values of the rate coefficients at the two temperatures and the values are in all cases slightly below the Langevin limit.

Table V shows values for the rate coefficients obtained from our dynamics calculations as well as data from laboratory measurements for reaction (1.1). Experimental studies provide rate coefficients for this reaction at temperatures in the range between 10–300 K.[5,7,9] The laboratory techniques employed vary from the ion cyclotron resonance (ICR) (see Ref. 32, cited in Ref. 9) and the VT-SIFT of the earlier studies,[5,7] to the low temperature multipole ion trap of the recent 10 K result.[9]

The most recently reported value of $3.5 \times 10^{-10}\,\mathrm{cm^3\,s^{-1}}$, measured at laboratory conditions that best resemble the interstellar cloud environment, is in apparent

TABLE V. Total rate coefficients for the reaction of $H_3^+ + HD$.

	k ($\mathrm{cm^3\,s^{-1}}$)			
T (K)	a	b	c	d
10	1.21 (−9)	1.21 (−9)	⋯	3.5 (−10)
80	1.13 (−9)	1.13 (−9)	1.2 (−9)	
300	1.08 (−9)	1.08 (−9)	9.6 (−10)	

[a]This work (using the MP2 interpolated PES).
[b]This work [using the CCSD(T)-MP2 interpolated PES].
[c]Experimental, uncertainty ±25%, see Ref. 7.
[d]Experimental, see Ref. 9.

contradiction to the earlier measurements, at higher temperatures, which seem to support a rate coefficient very close to the Langevin value for reaction (1.1) (i.e., $1.70 \times 10^{-9}\,cm^3\,s^{-1}$) at 10 K in the ISM.[5,7] There are important consequences of this rate coefficient value for models of the interstellar chemistry of deuterated species, discussed in Ref. 3, so an accurate theoretical value for this rate coefficient is worth pursuing.

Classical dynamics with the interpolated PES leads us to rate constants that are closer to the trend suggested by the earlier experimental results for reaction (1.1). The calculated rate coefficient at 10 K is not the Langevin limit but a lower value, which is nevertheless a factor of about 3.5 larger than the 10 K experimental value. We note that the classical rate coefficient for (1.1) is similar to the predicted values for reactions (1.2)–(1.3). The likely sources of error in these theoretical values are the use of classical mechanics and the *ab initio* approximation used to construct the PES.

In order to test the reliability of the *ab initio* approximation used to calculate the data points of the PES, we reevaluated the energies of all configurations of the PES data points at the CCSD(T) level and kept the MP2 gradients and Hessians to construct the CCSD(T) MP2 PES. Classical trajectory calculations for reaction (1.1) were performed on the CCSD(T) MP2 PES, with the same initial conditions used for the dynamics on the MP2 PES.

The dynamics upon the corrected CCSD(T) MP2 PES gives cross sections and rate coefficients for reaction (1.1) essentially the same as the values from dynamics on the MP2 PES. The two sets of cross sections could be fitted to logarithmic relationships as shown in Fig. 3. The fitting parameters for the MP2 PES based cross sections are printed in Fig. 3, while for the case of CCSD(T) based values they are slope $=-0.5322$, intercept 0.1677; $R^2=0.9941$. The rate coefficients for reaction (1.1) calculated using both relationships were the same at the three temperatures considered in Table V, at three significant digits precision.

Therefore, we can consider the classical dynamics with the MP2 interpolated PES as quantitatively correct and that a substantial correction to these classical results would only be likely due to quantum effects.

Assuming the exothermicity for reactions (1.1)–(1.3) to be approximately equal to the ZPVE released in these reactions, other authors (see Ref. 7, and references cited therein) have calculated the values +143 K for reaction (1.1), +251 K for reaction (1.2), and +63 K for reaction (1.3). There is a large ZPVE change for all processes considered, relative to a temperature of 10 K, and also for reactions (1.1) and (1.2), relative to 80 K. Note that there are no energy barriers for all these reactions, and hence no tunneling dynamics. Nonetheless, quantum dynamics in the collision complex at low energy may alter the cross sections as well as the branching ratios for channels (1.2) and (1.3) from their classical values. Clearly, quantum reactive scattering dynamics are required to determine an accurate theoretical value for the rate coefficient of reaction (1.1) at 10 K.

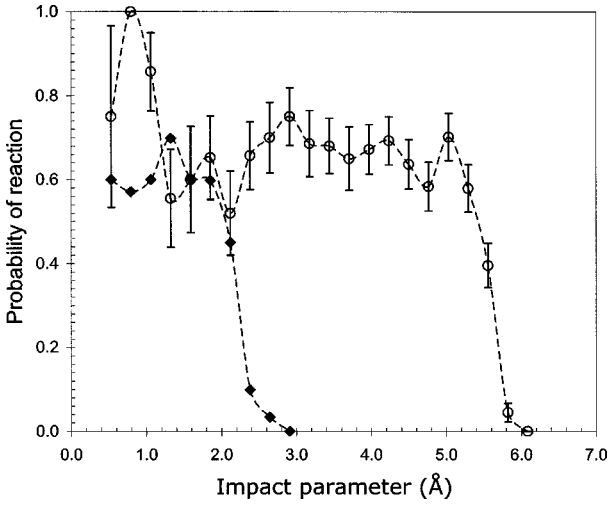

FIG. 5. A histogram of the reaction probability is presented as a function of the impact parameter, according to the classical dynamics, for the reaction of (a) $H_3^+ + D_2$, and (b) $H_3^+ + D_2$. Results for relative kinetic energies of the reactants $7.5\times10^{-4}\,E_h$ (○) and $5.0\times10^{-2}\,E_h$ (♦) are shown. The connecting lines are merely a visual aid. The error bars denote two standard deviations and, for clarity of presentation, are included only in one of the cases. The histograms were calculated with an impact parameter bin size of 0.26 Å.

C. Reaction mechanism

The total reaction probability $P(b)$ for (1.1), as a function of the impact parameter b, fluctuates around 0.7 for values of b up to a cutoff value. This cutoff impact parameter varies from approximately 2.9 Å at $E_{tr}=5.0\times10^{-2}\,E_h$ to 6.1 Å at $E_{tr}=7.5\times10^{-4}\,E_h$ as is shown in Fig. 5. The total reaction probability for (1.2) and (1.3) is similar, with a cutoff impact parameter which varies from 2.4 Å at $E_{tr}=5.0\times10^{-2}\,E_h$ to 5.8 Å at $E_{tr}=7.5\times10^{-4}\,E_h$ (see Fig. 6). In contrast, the Langevin model assumes an ion–molecule capture probability equal to unity[30] whenever the impact parameter is below a critical value of $b^*=(2\alpha e^2/E_{tr})^{1/4}$. According to this formula, b^* varies from 2.1 Å to 5.8 Å for reaction (1.1), and from 2.0 Å to 5.8 Å for reactions (1.2) and (1.3), at the energy limits indicated.

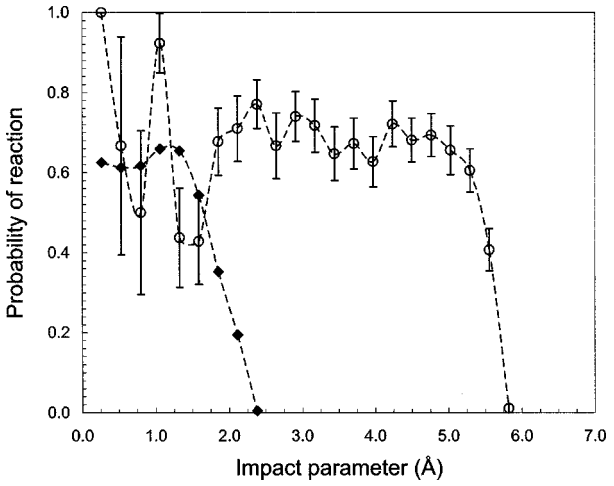

FIG. 6. As in Fig. 5, for reaction of $H_3^+ + HD$.

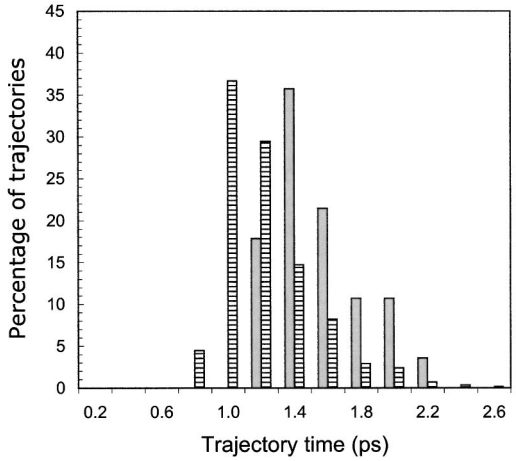

FIG. 7. Histograms of trajectory times for reaction (1.2), lined filled bars, and (1.3), solid bars, for a relative reactant kinetic energy of $1.0\times10^{-3}\ E_h$. Each percentage is relative to the number of trajectories following the corresponding channel. The histograms were calculated with a bin size of 0.2 ps.

If, below the cutoff values of *b*, the reactants are always captured in a five atom ion-complex, a total probability of reaction of about 0.7 implies that such a complex does not live long enough to allow the dissociation to proceed statistically, as if the hydrogen isotopes formed a fully random combination in the intermediate. In this limit, the combinatorial count would give a total probability of reaction equal to 0.9 for the reaction of $H_3^+ + D_2$, and 0.6 for the reaction of $H_3^+ + HD$. Furthermore, in a ''pure scrambling'' situation, the reaction probabilities for the two channels of the reaction of $H_3^+ + D_2$ would be 0.6 for channel $H_2D^+ + HD$ and 0.3 for channel $HD_2^+ + H_2$. However, both the present classical dynamics and experimental measurements differ significantly from the predictions of the scrambling mechanism. $HD_2^+ + H_2$ is the principal channel in the whole range of energies considered. Moreover, the reaction probabilities vary from 0.6 for product $HD_2^+ + H_2$, and 0.02 for product $H_2D^+ + HD$ at $E_{tr}=7.5\times10^{-4}\,E_h$ to 0.4 for product $HD_2^+ + H_2$, and 0.002 for product $H_2D^+ + HD$ at $E_{tr}=5.0\times10^{-2}\,E_h$.

The small probability predicted for reaction (1.3) in comparison with (1.2) could indicate that ''scrambling'' of the hydrogen isotopes happens to a very low extent over the energy range considered in the classical dynamics calculations, decreasing as the relative kinetic energy of the fragments increases. Figure 7 shows a histogram of the trajectory times for reactions (1.2) and (1.3) at $E_{tr}=1.0\times10^{-3}\,E_h$. Although Fig. 7 is calculated from 584 trajectories which produce $HD_2^+ + H_2$, and only 28 trajectories which produce $H_2D^+ + HD$, it is nevertheless clear that the latter trajectories are longer in time. The distribution peaks differ by about 0.4 ps, which indicates the additional time required for ''scrambling'' of the atoms in the collision complex. The higher probability of $H_2D^+ + HD$ products at lower collision energy implies that longer lived complexes are more common at lower relative translational energy. In conclusion, the formation of long-lived intermediate complexes does not appear to be important for the main reaction mechanism followed at relatively high temperatures, but could become relatively important when the temperature is as low as the average values in the ISM.

It is natural to ask what other factors could determine the calculated values of $P(b)$ below the cutoff impact parameter. There are long range contributions to the potential energy, not only from the charge-induced dipole term (which is taken as the potential in the Langevin model), but also relatively strong charge-quadrupole interactions. The latter interaction is dependent on the orientation of the neutral molecule, as previously discussed in relation to the dissociation of H_5^+ into H_3^+ and H_2.[18] This long range steric effect would result in repulsive forces for some orientations of the neutral molecule and could partially account for the differences between our predicted reaction probabilities and that of the Langevin model. That is, some fraction of trajectories at small impact parameters would not lead to capture in an ion–molecule complex. In addition, short range repulsive forces may be important. That is, even if the Langevin model conditions for ion–molecule capture are satisfied, the relative orientation of the colliding reactants is unfavorable for the reaction: Short range repulsion between the fragments leads to rapid dissociation of the ion–molecule pair before proton transfer can occur.

IV. SUMMARY AND CONCLUDING REMARKS

We have constructed two PES for the system H_5^+ and its isotopic analogs. The first is given by interpolation of MP2/6-311G(d,p) energy, gradients and Hessians calculated at 728 H_5^+ configurations. The second, a modified version of the former PES, is obtained by substituting CCSD(T)/6-311G(d,p) energy values for the MP2 values at the same 728 points. The CCSD(T)-MP2 PES gives a dissociation energy for H_5^+, according to reaction (2.2), within 3.5 kJ mol^{-1} of the most reliable *ab initio* results available.

A classical dynamics study on both the MP2 PES and CCSD(T)-MP2 PES yields cross sections and rate coefficients for reactions (1.1) and (1.2)–(1.3) in agreement with earlier experimental results and in qualitative agreement with the Langevin model. The quantitative agreement between the classical cross sections on the two surfaces suggests that the PES is effectively converged with respect to the level of electronic structure calculation. According to the classical dynamics, the predicted reaction probabilities differ from those corresponding to a totally combinatorial distribution of the atoms involved. Hence, reaction (1.1) and its isotopic analogs proceed by a mechanism which does not involve long-lived five atom complexes for relative translational energies of the reactants between 7.5×10^{-4} and $5.0\times10^{-2}\,E_h$. However, the predicted rate constant for reaction (1.1) at a temperature of 10 K is considerably higher than the most recent experimental data. This fact, together with the obvious importance of zero point energy effects at low energy, suggests the necessity for quantum scattering calculations.

The data files and software necessary to evaluate the PES are available from the authors upon request or as EPAPS documents.[33]

ACKNOWLEDGMENT

The authors wish to thank the Australian Partnership for Advanced Computing National Facility for an allocation of computer time.

[1] T. J. Millar, Planet. Space Sci. **50**, 1189 (2002).
[2] J. Tennyson, Rep. Prog. Phys. **58**, 421 (1995).
[3] H. Roberts, E. Herbst, and T. J. Millar, Mon. Not. R. Astron. Soc. **336**, 283 (2002).
[4] D. Gerlich and S. Schlemmer, Planet. Space Sci. **50**, 1287 (2002).
[5] N. G. Adams and D. Smith, Astrophys. J. **248**, 373 (1981).
[6] C. H. Douglass, G. Ringer, and W. R. Gentry, J. Chem. Phys. **76**, 2423 (1982).
[7] K. Giles, N. G. Adams, and D. Smith, J. Phys. Chem. **96**, 7645 (1992).
[8] M. L. Vestal, C. R. Blakley, P. W. Ryan, and J. H. Futrell, J. Chem. Phys. **64**, 2094 (1976).
[9] D. Gerlich, E. Herbst, and E. Roueff, Planet. Space Sci. **50**, 1275 (2002).
[10] S. A. Sandford, Planet. Space Sci. **50**, 1145 (2002).
[11] R. Ahlrichs, Theor. Chim. Acta **39**, 149 (1975).
[12] P. Bokes, I. Stich, and L. Mitas, Int. J. Quantum Chem. **83**, 86 (2001).
[13] H. Chermette, H. Razafinjanahary, and L. Carrion, J. Chem. Phys. **107**, 10643 (1997).
[14] H. Muller and W. Kutzelnigg, Phys. Chem. Chem. Phys. **2**, 2061 (2000).
[15] Y. Yamaguchi, J. F. Gaw, and H. F. Schaefer, J. Chem. Phys. **78**, 4074 (1983).
[16] E. W. Ignacio and S. Yamabe, Chem. Phys. Lett. **287**, 563 (1998).
[17] M. Barbatti, G. Jalbert, and M. A. C. Nascimento, J. Chem. Phys. **113**, 4230 (2000).
[18] R. Prosmiti, A. A. Buchachenko, P. Villarreal, and G. Delgado-Barrio, Theor. Chem. Acc. **106**, 426 (2001).
[19] V. Spirko, W. P. Kraemer, and P. Soldan, J. Mol. Spectrosc. **183**, 218 (1997).
[20] M. A. Collins, Theor. Chem. Acc. **108**, 313 (2002).
[21] J. Ischtwan and M. A. Collins, J. Chem. Phys. **100**, 8080 (1994); M. J. T. Jordan, K. C. Thompson, and M. A. Collins, *ibid.* **103**, 9669 (1995).
[22] M. J. T. Jordan, K. C. Thompson, and M. A. Collins, J. Chem. Phys. **102**, 5647 (1995); K. C. Thompson and M. A. Collins, J. Chem. Soc., Faraday Trans. **93**, 871 (1997).
[23] R. P. A. Bettens and M. A. Collins, J. Chem. Phys. **111**, 816 (1999).
[24] K. Hiraoka, J. Chem. Phys. **87**, 4048 (1987).
[25] K. Hiraoka and T. Mori, J. Chem. Phys. **91**, 4821 (1989).
[26] M. Yang, D. H. Zhang, M. A. Collins, and S. Y. Lee, J. Chem. Phys. **114**, 4759 (2001).
[27] G. W. Frisch, G. W. Trucks, H. B. Schlegel *et al.*, GAUSSIAN 98 Gaussian, Inc., Pittsburgh, PA, 1998.
[28] M. P. Allen and D. J. Tildesley, *Computer Simulations of Liquids* (Clarendon, Oxford, 1987).
[29] H. W. Schranz, S. Nordholm, and G. Nyman, J. Chem. Phys. **94**, 1487 (1991).
[30] J. I. Steinfeld, J. S. Francisco, and W. L. Hase, *Chemical Kinetics and Dynamics* (Prentice–Hall, Englewood Cliffs, 1989).
[31] J. Rychlewski, Mol. Phys. **41**, 833 (1980).
[32] W. T. Huntress and V. G. Anicich, Astrophys. J. **208**, 237 (1976).
[33] See Document No. E-JCPSA6-119-306335 for the data file and software to evaluate the PES. A direct link to this document may be found in the online article's HTML reference section. The document may also be reached via the EPAPS homepage (http://www.aip.org/pubservs/epaps.html) or from ftp.aip.org in the directory /epaps/. See the EPAPS homepage for more information.